MoS_2 hierarchical hollow cubic cages assembled by bilayers: one-step synthesis and their electrochemical hydrogen storage properties†

Lina Ye, Changzheng Wu, Wen Guo and Yi Xie*

Received (in Cambridge, UK) 24th July 2006, Accepted 5th September 2006
First published as an Advance Article on the web 26th September 2006
DOI: 10.1039/b610601c

Micrometer scaled MoS_2 hierarchical hollow cubic cages assembled by bilayers can be synthesized *via* a one-step self-assembly coupled with intermediate crystal templating process without any surfactant, in which the intermediate $K_2NaMoO_3F_3$ crystal formed *in-situ* and then served as the self-sacrificed template based on the Kirkendall Effect; The MoS_2 hierarchical hollow cubic cages were employed for electrochemical hydrogen storage with a high capacity of 375 mAh g^{-1} due to the more active edges exposing on the upright-standing nanoplates.

Over the last few years, synthetic fabrication of hierarchical hollow nanostructures has attracted significant interest[1–4] due to their widespread potential applications in catalysis, drug delivery, lightweight filter, acoustic insulation, photonic crystals,[5] and so on. However, in most cases, only spherical hierarchical hollow structures could be synthesized through the use of emulsion droplets[1] as templates, or by direct self-assembly of primary particles without using external templates.[2–4] Recently, rhombo-dodecahedral silver cages have been prepared by the self-assembly coupled with precursor crystal templating approach,[6] which involved a two-step process. Precursor Ag_3PO_4 crystal was first synthesized, with surfactant being used as a crystal-growth modifier. After being separated from the surfactant solution, the precursor was washed and then reacted with reducing agent to form Ag cages. Thus it is desirable to explore facile methods with one-step surfactant-free approach to organize primary building blocks into hollow cages with well defined, novel geometrical morphologies.

MoS_2, due to its layered structure, which consists of covalently bound S–Mo–S trilayers separated by a relatively large van der Waals gap[7] has attracted considerable attention for its interesting properties and important applications such as electrochemical hydrogen storage, solid lubricants, solid-state secondary lithium battery cathodes, magnesium batteries and industrial catalysts for hydrodesulfurization of crude oil.[8–12] Considerable effort has been devoted to MoS_2 nanowires,[13] nanotubes,[14] nanoribbons,[15] bubbles,[16] and porous structures[17] by employing techniques such as hydrothermal, gas–solid reaction, MOCVD, electrochemical/chemical method, sonochemical synthesis, and ultrasonic spray pyrolysis. It is known that inorganic materials always show unique size- and shaped-dependent properties, for example, Chen found MoS_2 morphology exerted a noticeable influence on the electrochemical hydrogen storage ability,[8] which inspired us to search for a simple, inexpensive, and efficient approach to the morphology-controlled synthesis of MoS_2 nanostructures/microstructures, especially those with novel and interesting morphologies. Herein we report the synthesis of MoS_2 hierarchical hollow cubic cages assembled by bilayers through a one-step self-assembly coupled with intermediate crystal templating process without any surfactant.

In a typical procedure, NaF (0.012 mol), MoO_3 (0.006 mol), and KSCN (0.018 mol) powders were added into 30 mL of distilled water and transferred to a Teflon-lined stainless steel autoclave, which was then heated at 220 °C for 24 hours in an electric oven. After reaction, the black precipitate was filtered and washed several times with distilled water and anhydrous alcohol. The final product was dried in a vacuum at 60 °C for 6 hours. Our XRD study of the final product (Fig. 1A) is consistent with the previous report[18] and indexed to hexagonal phase of MoS_2 with lattice parameters $a = 3.151(4)$ Å and $c = 12.78(6)$ Å respectively.‡

From FESEM observations, we find that this facile route at 220 °C for 24 h results in the formation of a great deal of uniform MoS_2 cages with well-preserved cubic morphology. The cubic cages have an edge-length ranging from 1 to 2 μm (Fig. 2A) and exhibit rather rough surfaces (Fig. 2B). The interior space of the hollow MoS_2 cubic cages is clearly revealed on the FESEM image

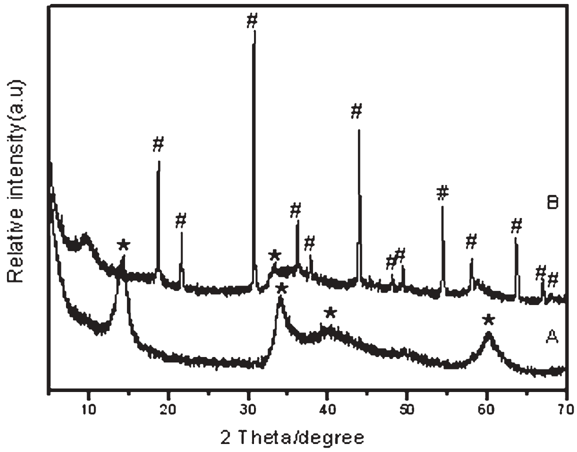

Fig. 1 XRD patterns: (A) the final product of MoS_2 (*), (B) the intermediate product of $K_2NaMoO_3F_3$ (#) with the coexistence of minor MoS_2 (*).

Department of Nanomaterials and Nanochemistry, Hefei National Laboratory for Physical Sciences at Microscale, University of Science and Technology of China, Hefei 230026, P. R. China.
E-mail: yxie@ustc.edu.cn; Fax: 86-551-3603987

† Electronic supplementary information (ESI) available: FESEM images of the intermediate $K_2NaMoO_3F_3$, the bilayer structure, and the products prepared without using NaF or with high-concentration NaF starting solution, and electrochemical hydrogen storage results. See DOI: 10.1039/b610601c

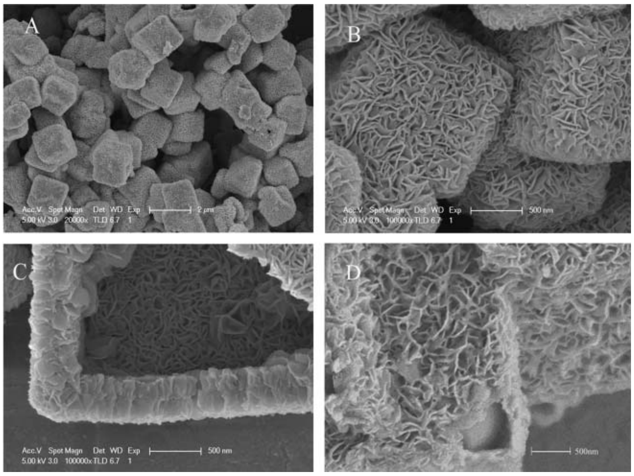

Fig. 2 FESEM images of MoS_2 hollow cubic cages: (A) overall product morphology; (B) detailed view of the surface of the cubic cages; (C) a detailed view of an incomplete cubic cage, showing its hollow interior and the shell of the cubic cages consisting of irregular-shaped, upright-standing bilayers about 400 nm in thickness; (D) a broken intermediate sample collected at 220 °C for 2.5 h while other experiment conditions remain the same, from which we can see a thin loose MoS_2 shell clearly covering the solid $K_2NaMoO_3F_3$ core.

for an incomplete MoS_2 cubic cage (Fig. 2C). It can be seen that the shell of the cubic cages consists of irregular-shaped, upright-standing bilayers about 400 nm in thickness.

In our approach, this formation of micrometer-sized cubic cages is believed to be the result of the Kirkendall Effect,[19] which was first introduced to nanomaterial synthesis and then well explained by Xia's group.[19a,b] While the formation of MoS_2 nanoplates mainly lies on the MoS_2 lamellar (2D) structure, the key point in our synthesis of MoS_2 hierarchical hollow cubic cages involves the *in-situ* formation of intermediate $K_2NaMoO_3F_3$ cubic crystals in aqueous solution, which then serve as a self-sacrificing template in the subsequent reaction with S^{2-} released from SCN^- upon a hydrolyzation process. Thus the whole process can be simply described as a self-assembly coupled with intermediate crystal templating process (Scheme 1).

In this process, bulky MoO_3 particles react with Na^+, K^+ and F^- to form cubic $K_2NaMoO_3F_3$[20] under the hydrothermal treatment, and at the same time, S^{2-} released from SCN^- upon a hydrolyzation process in this system. As $K_2NaMoO_3F_3$ can be readily reduced and sulfuretted by S^{2-} to MoS_2, the *in-situ* forming $K_2NaMoO_3F_3$ cubic crystals may be used as the intermediate for the morphology-preserved synthesis of MoS_2. In the present case, $K_2NaMoO_3F_3$ and S^{2-} can react with each other and form a diffusion pair, the coupled reaction–diffusion at the crystal–solution interface could lead to the quick formation of an interconnected MoS_2 shell around the external surfaces of the $K_2NaMoO_3F_3$ crystals. This process is followed by a continuous outward flow of $K_2NaMoO_3F_3$ from the solution to and through the porous MoS_2 shell to form a hollow interior and a relatively compact shell. As further evidence, the intermediate $K_2NaMoO_3F_3$–MoS_2 core–shell structure has been indeed collected in our experiments in which the reagents reacted for a shorter time (*e.g.*, 220 °C, 2.5 h). XRD study (Fig. 1B) shows that the intermediate is cubic $K_2NaMoO_3F_3$ (JCPDS File No.74-0297) with the coexistence of minor MoS_2. Fig. 2D and Fig. S1† show a typical FESEM image of the intermediate $K_2NaMoO_3F_3$ core with the layer of MoS_2 shell, in which a thin loose MoS_2 shell made up of many upstanding nanoplates is clearly covering the solid $K_2NaMoO_3F_3$ core. While the sacrificing templating effect of the intermediate $K_2NaMoO_3F_3$ is well understood, the formation of the bilayer structure is surprising. However, it is still in accordance with the Kirkendall effect because significant inward S^{2-} transport could occur after the initial formation of the shell around the cubic intermediate crystals,[6] thus upstanding MoS_2 nanoplates would form on the internal surface of the preformed MoS_2 shell (as shown in Fig. S2†). All the above confirmed the $K_2NaMoO_3F_3$ really formed *in-situ* in the process and then served as a self-sacrificing template for the final cubic morphology of MoS_2 hollow cages.

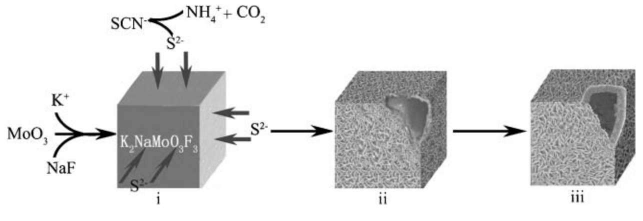

Scheme 1 Schematic illustration of formation of MoS_2 hollow cubic cages: (i) intermediate $K_2NaMoO_3F_3$ cubic crystal, (ii) the intermediate $K_2NaMoO_3F_3$ core with the layer of MoS_2 shell structure, (iii) continuous evacuation of intermediate $K_2NaMoO_3F_3$ core and growth of MoS_2 bilayer shell assembled by many nanoplates.

It has been revealed that the intermediate cubic $K_2NaMoO_3F_3$ is crucial to the formation of morphology-preserved MoS_2 cubic cages. Our comparison experiments indicate that using NaSCN as the sulfur source instead of KSCN would eliminate the desirable growth of cubic $K_2NaMoO_3F_3$ in absence of initial K^+, giving the final unorganized MoS_2 nanoplates. In addition, introducing NaF to the starting solution is a prerequisite to form cubic $K_2NaMoO_3F_3$. Our contrastive experiments showed that flower-like MoS_2 assembled by nanoplates were formed in the absence of NaF (Fig. S3-1†). Nonetheless, an exceeding high concentration of starting NaF would promote the spontaneous nucleation and growth of intermediate $K_2NaMoO_3F_3$ cube, resulting in the larger MoS_2 cubic cages (Fig. S3-2†). All the above further confirm the proposed mechanism in Scheme 1.

MoS_2 shows the electrochemical hydrogen storage ability due to its lamellar structure[8] based on the charge-transfer reaction and diffusion step (Scheme 2).

It has been found that only the edges of MoS_2 sheet where the sulfur atom, which binds the hydrogen, is 2-fold coordinated to metal atoms are interesting in binding to atomic hydrogen, as the basal plane of MoS_2 is catalytically inactive.[21,22] In our approach, as the shell of the MoS_2 hierarchical hollow cubic cages consists of bilayers assembled by many irregular-shaped, upright-standing nanoplates, thus more edges are exposed, hence our products are expected to possess a higher electrochemical charging capacity. The results of electrochemical hydrogen storage experiments come up to our expectations.

$$H_2O+MoS_2+e^- \underset{Ox}{\overset{Red}{\rightleftharpoons}} H_{ad}/MoS_2+OH^- \underset{Diff}{\overset{Diff}{\rightleftharpoons}} H_{ab}/MoS_2+OH^-$$

Scheme 2 Electrochemical hydrogen storage of MoS_2.

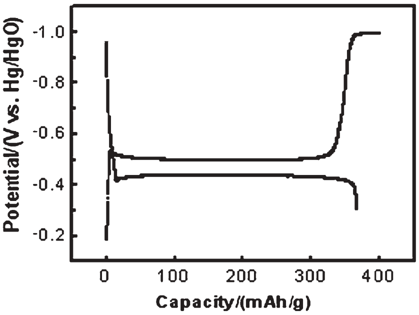

Fig. 3 Charge and discharge curve of the as-prepared MoS_2 electrode at a constant current of 100 mA g^{-1}.

The charge–discharge curves displayed by the electrodes made of the as-prepared MoS_2 cubic cages showed the electrochemical charging capacity of 375 mAh g^{-1} at 50 mA g^{-1} (Fig. S4-1†), 356 mAh g^{-1} at 100 mA g^{-1} (Fig. 3) and 324 mAh g^{-1} at 200 mA g^{-1} (Fig. S4-2†), comparable to the value of 260 mAh g^{-1} at 50 mA g^{-1}, 225 mAh g^{-1} at 100 mA g^{-1} and 178 mAh g^{-1} at 200 mA g^{-1} reported for the MoS_2 nanotubes[8] respectively, implying a potential application in electrochemical hydrogen storage.§

In summary, micrometer scaled MoS_2 hierarchical hollow cubic cages assembled by bilayers can be constructed *via* a one-step intermediate crystal templating process without surfactant, where the intermediate cubic $K_2NaMoO_3F_3$ forms *in-situ* and subsequently serves as a self-sacrificial template for the initial nucleation and growth of MoS_2. The as-prepared MoS_2 hierarchical hollow cubic cages can be electrochemically charged and discharged with a high capacity of 375 mAh g^{-1} due to the more active edges exposing on the upright-standing nanoplates. Furthermore, the synthesis may be extended to other sulfide systems and could be used for device fabrication with appropriate intermediate/sulfur source combinations.

This work was financially supported by the National Natural Science Foundation of China (No. 20321101) and the state key project of fundamental research for nanomaterials and nanostructures (2005CB623601).

Notes and references

‡ The sample of the as-prepared MoS_2 was characterized by X-ray powder diffraction (XRD) with a Japan Rigaku D/max rA X-ray diffractometer with Ni-filtered Cu Kα radiation (λ = 1.5418 Å). The field emission scanning electron microscopy (FESEM) images were taken on a FEI Sirion-200 SEM.

§ The electrochemical hydrogen storage experiments were performed in a three-electrode system in 6 M KOH at 25 °C under ambient pressure (using the Land battery system CT2001A). MoS_2 sample was used as working electrode, $Ni(OH)_2$/NiOOH as the counter electrode, and Hg/HgO as reference electrode. Working electrode was prepared by mixing 20 mg of the MoS_2 sample with 60 mg of Cu powder and being directly pressed on a sheet of nickel foam at 40 MPa. The electrodes made of the as-prepared MoS_2 cubic cages were charged–discharged at constant current density of 50 mA g^{-1} (charged–discharged for 8 hours), 100 mA g^{-1} (charged–discharged for 4 hours) and 200 mA g^{-1} (charged–discharged for 2 hours).

1 A. D. Dinsmore, M. F. Hsu, M. G. Nikolaides, M. Marquez, A. R. Bausch and D. A. Weitz, *Science*, 2002, **298**, 1006.
2 A. Bigi, E. Boanini, D. Walsh and S. Mann, *Angew. Chem., Int. Ed.*, 2002, **41**, 2163.
3 J. Yuan, K. Laubernds, Q. Zhang and S. L. Suib, *J. Am. Chem. Soc.*, 2003, **125**, 4966.
4 B. Liu and H. C. Zeng, *J. Am. Chem. Soc.*, 2004, **126**, 8124–8125.
5 F. Caruso, *Chem.–Eur. J.*, 2000, **6**, 413.
6 Y. J. Yang, L. M. Qi, C. H. Lu, J. M. Ma and H. M. Cheng, *Angew. Chem., Int. Ed.*, 2005, **44**, 598–603.
7 (*a*) R. G. Dickinson and L. Pauling, *J. Am. Chem. Soc.*, 1923, **45**, 1466; (*b*) R. Tenne, *Adv. Mater.*, 1995, **7**, 965.
8 J. Chen, N. Kuriyama and H. T. Yuan, *J. Am. Chem. Soc.*, 2001, **123**, 11813–11814.
9 (*a*) M. Chhowalla and G. A. J. Amaratunga, *Nature*, 2000, **407**, 164–167; (*b*) L. Rapoport, Y. Bilik, Y. Feldman, M. Homyonfer, S. R. Cohen and R. Tenne, *Nature*, 1997, **387**, 791–793.
10 N. Imanishi, K. Kanamura and Z. Takehara, *J. Electrochem. Soc.*, 1992, **139**, 2082–2087.
11 (*a*) D. Aurbach, Z. Lu, A. Schechter, Y. Gofer, H. Gizbar, R. Turgeman, Y. Cohen, M. Moshkovich and E. Levi, *Nature*, 2000, **407**, 724; (*b*) Z. Lu, A. Schechter, M. Moshkovich and D. Aurbach, *J. Electroanal. Chem.*, 1999, **466**, 203; (*c*) O. Chusid, Y. Gofer, H. Gizbar, Y. Vestfrid, E. Levi, D. Aurbach and I. Riech, *Adv. Mater.*, 2003, **15**, 627; (*d*) X. L. Li and Y. D. Li, *J. Phys. Chem. B*, 2004, **108**, 13893–13900.
12 (*a*) J. Chen, S. L. Li, Q. Xu and K. Tanaka, *Chem. Commun.*, 2002, 1722–1723; (*b*) S. E. Skrabalak and K. S. Suslick, *J. Am. Chem. Soc.*, 2005, **127**, 9990–9991.
13 W. J. Li, E. W. Shi, J. M. Ko, Z. Z. Chen, H. Ogino and T. Fukuda, *J. Cryst. Growth*, 2003, **250**, 418–422.
14 (*a*) J. Chen, S. L. Li, Q. Xu and K. Tanaka, *Chem. Commun.*, 2002, 1722–1723; (*b*) M. Nath, A. Govindaraj and C. N. R. Rao, *Adv. Mater.*, 2001, **13**, 283–286; (*c*) K. P. Loh, H. Zhang, W. Z. Chen and W. Ji, *J. Phys. Chem. B*, 2006, **110**, 1235–1239.
15 Q. Li, J. T. Newberg, E. C. Walter, J. C. Hemminger and R. M. Penner, *Nano Lett.*, 2004, **4**, 277–281.
16 I. Uzcanga, I. Bezverkhyy, P. Afanasiev, C. Scott and M. Vrinat, *Chem. Mater.*, 2005, **17**, 3575–3577.
17 S. E. Skrabalak and K. S. Suslick, *J. Am. Chem. Soc.*, 2005, **127**, 9990–9991.
18 T. P. Prasad, E. Diemann and A. Müller, *J. Inorg. Nucl. Chem.*, 1973, **35**, 1895–1904.
19 (*a*) Y. G. Sun and Y. N. Xia, *Science*, 2002, **298**, 2176; (*b*) Y. D. Yin, R. M. Rioux, C. K. Erdonmez, S. Hughes, G. A. Somorjai and A. P. Alivisatos, *Science*, 2004, **304**, 711; (*c*) Y. L. Wang, L. Cai and Y. N. Xia, *Adv. Mater.*, 2005, **17**, 473; (*d*) B. Liu and H. C. Zeng, *J. Am. Chem. Soc.*, 2004, **126**, 16744; (*e*) H. L. Cao, X. F. Qian, C. Wang, X. D. Ma, J. Yin and Z. K. Zhu, *J. Am. Chem. Soc.*, 2005, **127**, 16024–16025.
20 G. Pausewang and W. Z. Ruedorff, *Z. Anorg. Allg. Chem.*, 1969, **364**, 69.
21 P. Raybaud, J. Hafner, G. Kresse, S. Kasztelan and H. Toulhoat, *J. Catal.*, 2000, **189**, 129.
22 B. Hinnemann, P. G. Moses, J. Bonde, K. P. Jørgensen, J. H. Nielsen, S. Horch, I. Chorkendorff and J. K. Nørskov, *J. Am. Chem. Soc.*, 2005, **127**, 5308–5309.